Egypt. J. Chem. **Vol. 66**, No. **SI, 13, 1373-1382** (2023)

Egyptian Journal of Chemistry

http://ejchem.journals.ekb.eg/

Nano Co(II) and Pd(II) Schiff base Complexes: Structural Characterization, Molecular docking, Antitumor proficiency and Biological evaluation

Omnia M.Fahmy [1], Walaa H. Mahmoud [1] , Rasha M. Elnashar [1] and Ahmed A. El-Sherif [1]

[1] Department of Chemistry, Faculty of Science, Cairo University, Egypt

*Correspondence: aelsherif@sci.cu.edu.eg (Prof. Dr. Ahmed El-Sherif);

Abstract

new Schiff base ligand (L) formed from benzotriazole and phethalazine moieties was developed and used to synthesize the mononuclear metal complexes [$CoLCl_2$] and [$PdLCl_2$]. Elemental analyses, FT-IR, mass spectra, NMR spectral studies, SEM, and conductivity tests were all used to comprehensively identify the chemical structures of produced compounds. The prepared ligand and its complexes' nanostructures were confirmed by SEM analysis. The synthesized ligand and its M(II) complexes' antibacterial effects on bacterial (positive and negative) and fungal strains were investigated. The early in vitro antibacterial and antifungal screening activities showed that complexes had somewhat stronger antibacterial and antifungal activity than the ligand and showed moderate activity against the tested pathogens. The Schiff base ligand and its metal complexes were tested for anticancer efficacy against human cancer (MCF-7 and HepG2 cell viability). In comparison to breast and liver cell lines, the Pd(II) complex displays increased activity with a lower IC_{50}. Molecular docking was utilized to predict the interaction between Schiff base ligand (L) and various receptors. To study inhibition, the docking investigation produced useful structural data.

Keywords: Schiff base; spectra; SEM; antimicrobial activity; anticancer; docking.

1. Introduction Due to their bio-medicinal capabilities, such as antibacterial, antifungal, antioxidant, anti-inflammatory, anticancer, and herbicidal actions, Schiff bases and their metal complexes constitute a prominent group of physiologically active compounds [1-3]. Due to their wide range of applications, including their ability to bind to DNA, their capacity for DNA cleavage, their catalytic and biological properties, their simplicity in synthesis, and their adaptable structural confirmations, metal complexes with Schiff bases play a significant role in coordination chemistry [4–8]. A significant part of numerous metabolic processes in living organisms is played by the biologically active cobalt ion. As a key metal ion, vitamin B12 controls how the brain and nervous system operate normally. According to earlier investigations, the majority of cobalt complexes significantly act as antioxidants, antimicrobials, antiproliferents, and antiviral medicines [9–19]. The

*Corresponding author e-mail: aelsherif@sci.cu.edu.eg/ aelsherif72@yahoo.com (Ahmed El-Sherif)
Received date 2023-01-10; revised date 2023-04-13; accepted date 2023-05-25
DOI: **10.21608/EJCHEM.2023.186272.7435**

literature review found that palladium complexes are effective anticancer and antibacterial agents. Therefore, the development of prospective medications with effective anticancer capabilities is crucial for fast treatments for various types of miscellaneous [20–23]. The primary goal of this research is to synthesize and characterize the Schiff base (L) ligand and its complexes with Co(II) and Pd(II) to better understand how the chelate system affects physicochemical characteristics and various biomedical applications.

2. Materials and methods

2.1.Experimental

2.1.1. Chemicals and reagents

The highest purity analytical grade (AR) chemicals were employed in all applications. They included 1-hydrazinylphthalazine and 1-(2H-benzo[d][1,2,3]triazol-2-yl]propan-2-one (Merck). We purchased the metal salts K_2PdCl_4 and $CoCl_2.6H_2O$ from Sigma-Aldrich and Merck, respectively. Dimethylformamide (DMF) and ethyl alcohol (99% each) were utilized as organic solvents. In all preparations, de-ionized water that was gathered from all glass equipment was typically used. The American Type Culture Collection provided the human tumor cell lines HepG2 and MCF-7, which were obtained frozen in liquid nitrogen (−180 °C). Serial subculturing was used to preserve the tumor cell lines at the National Cancer Institute in Cairo, Egypt.

2.1.2. Solutions

A precisely weighed quantity of the chelates was dissolved in the appropriate amount of ethanol to create fresh stock solutions of mixed ligand complexes of 1×10^{-3} M. Following that, the conductivity of each complex solution was determined. The suggested approaches were used to standardize the metal salt solutions [24, 25]. In order to measure UV-vis spectra, solutions of 1×10^{-4} M of the Schiff base ligand and its complexes were also prepared by diluting the prior stock solutions.

2.1.3. Instrumentation

A CHNS-932 (LECO) Vario elemental analyzer was used to provide microanalyses of carbon, hydrogen, and nitrogen at Cairo University's Microanalytical Center in Egypt. Triforce's XMTD-3000 was used to measure the melting point. KBr discs were used to record Fourier-transform infrared spectroscopy (FT-IR) spectra on a Perkin-Elmer 1650 spectrometer (4000–400 cm^{-1}). Tetramethylsilane served as an internal standard while ^1H NMR spectra were captured using a 300 MHz Varian-Oxford Mercury as solutions in DMSO-*d6* at ambient temperature. The magnetic susceptibilities were measured on powdered materials using the Faraday method. The molar conductivity of 10^{-3} M solutions of solid complexes in ethanol was measured using a Jenway 4010 conductivity meter. used Hewlett-Packard MS-5988 GS-MS equipment was used to record mass spectra at 70 eV using the electron ionization technique at the Microanalytical Center, Egypt. An automated spectrophotometer UV-vis Perkin-Elmer Model Lambda 20 ranging from 200 to 700 nm was used to perform the spectrophotometric measurements in solution. The antimicrobial measurements were performed at the Microanalytical Center at Cairo University in Egypt. The anticancer activity experiments were carried out at the National Cancer Institute, Department of Cancer Biology, Department of Pharmacology, Cairo University, Egypt. Using an ELIZA microplate reader (Meter tech. R960, USA) was used to spectrophotometrically determine the optical density (OD) of each well at 564 nm. Quanta FEG250 instrument was used to capture scanning electron microscopy (SEM) images of the ligand and its complexes at the National Research Center, Egypt.

2.2.Procedures

2.2.1.Synthesis of the Schiff base ligand [L]

By using the suggested technique, a novel Schiff base ligand was synthesized. The reaction was carried out by condensation of 1-hydrazinylphthalazine (5.68 mmol, 0.91 g), which was dissolved in hot absolute ethanol (60 °C), and 1-(2H-benzo[d][1,2,3]triazol-2-yl)propan-2-one (5.68 mmol, 1 g), which was dissolved in hot ethanol in a 1:1 molar ratio. The reaction mixture was then left under reflux for 4 h. Then a reddish-brown solid compound was separated after evaporation, and then the precipitate was filtered off and recrystallized from DMF–ethanol mixture to give pure Schiff base with 88% yield. Scheme (1) presents the general formation reaction mechanism and structure of the Schiff base ligand.

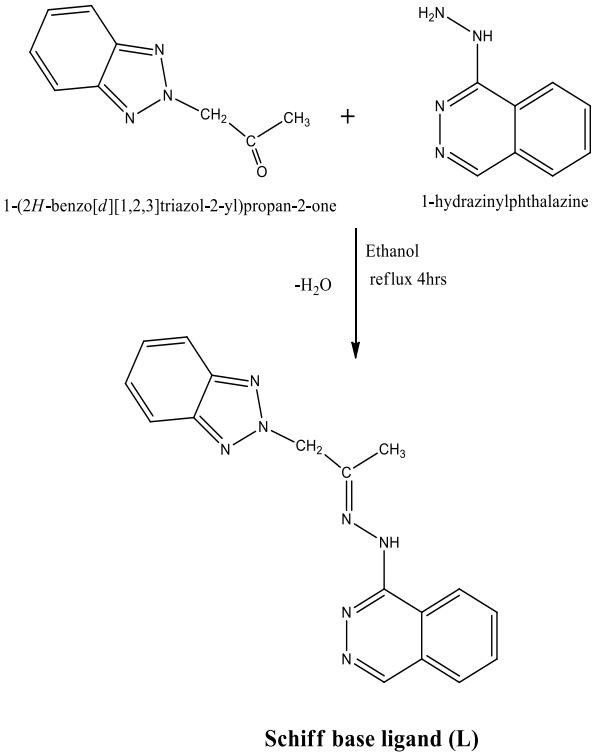

Scheme. 1: Synthesis pathway of the Schiff base ligand (L).

2.2.2. Synthesis of the metal complexes

A 20 ml hot ethanolic solution (70 °C) of the Schiff base ligand (1.58 mmol, 0.5 g) was mixed with 20 ml hot absolute ethanol of metal salts (1.58 mmol, 0.43 g, $CoCl_2.6H_2O$, and 0.52 g, K_2PdCl_4) to yields the metal complexes. Subsequently, the complexes precipitated after 3 hours of reflux-stirring the resultant mixture. It was then refined by washing it numerous times, collected by filtration, and dried in a vacuum over anhydrous calcium chloride. The complexes of pure metal were produced via recrystallization.

2.3.Antimicrobial activity

Gram-positive and Gram-negative bacteria (*Bacillus subtilis* and *Staphylococcus aureus*), Gram-positive bacteria (*Escherichia coli* and *Neisseria gonorrhoeae*), and fungus strains were used to evaluate the *in-vitro* antibacterial and antifungal activities of the synthesized complexes [26, 27]. Gentamycin was used as a positive control against Gram-negative bacteria, ampicillin for Gram-positive bacteria, and amphotericin (*Candida albicans*). By dissolving the Schiff base ligand and its complexes in DMSO, a stock solution (1 mmol) was obtained accordingly. After being prepared and cooled to 47 °C, the nutrient agar medium for an antibiotic was seeded with the studied microorganisms. After solidification, a sterile cork borer was used to drill 5 mm in diameter holes. The examined compounds, i.e., Schiff base ligand and its metal complexes, were introduced in Petri-dishes (only 0.1 m) after dissolving in DMSO at 1 x 10^{-3} M. These culture plates were then incubated at 37 °C for 20 h for bacteria. The diameter of the inhibition zones was measured in millimeters. Antimicrobial activities were performed in triplicate and the average was taken as the final reading [28]. The investigated compounds, namely the Schiff base ligand and its metal complexes, were dissolved in DMSO at a concentration of 1 x 10^{-3} M and then added to Petri plates (only 0.1 m). Then, these culture plates were cultured for bacteria for 20 hours at 37 °C. The inhibitory zones' diameter was measured in millimeters. The antimicrobial activities experiments were conducted in triplicate, and the average served as the final reading [28].

2.4. Anti-tumor activity

The Skehan and Storeng approach was used to examine the compound's potential cytotoxicity [29, 30]. Prior to treatment with the chemicals, cells were plated on a 96-multiwell plate with 104 cells per well for 24 h to allow for the attachment of the cell to the plate wall. For each dose, triplicate wells were made and three different concentrations of the chemicals under investigation (0, 5, 12.5, 25, 50, and 100 g/mL) were applied to the cell monolayer. The compounds were treated with the monolayer cells for 48 hours at 37 °C and in a 5% CO_2 environment. Cells were fixed, cleaned, and stained with SRB stain after 48 hours. Acetic acid was used to remove any excess stain, and Tris-EDTA buffer was used to remove any adhered stain. The optical density (O.D.) of each well was determined spectrophotometrically at 564 nm using an ELIZA microplate reader. The mean background absorbance was then automatically subtracted, and the mean values of each drug concentration were calculated. To determine the breast tumour cell line survival curve for each substance, a relationship between surviving fraction and drug concentration was shown. The following formula was used to compute the percentage of cells that survived:

$$\text{Survival fraction} = \frac{\text{O. D. (treated cells)}}{\text{O. D. (control cells)}}$$

The IC_{50} values (the concentrations of (L) ligand or its mixed ligand complexes required to produce 50% inhibition of cell growth). The experiment was repeated 3 times.

2.5.Molecular docking

Molecular docking studies were very significant for prophesying the possible binding modes of the most active compounds with the

receptors of the crystal structure of nucleoside diphosphate kinase of *Staphylococcus aureus* (3Q8U), the crystal structure of *E. coli* (3t88), protein phosphatase of fungus *Candida albicans* (5JPE) and with the crystal structure of breast cancer receptor (3HB5). These tests were also carried out to determine the inhibitor's binding free energy inside the macromolecule [31, 32]. They were carried out using the MOE 2008 program (MOE source: Chemical Computing Group Inc., Quebec, Canada, 2008), an interactive molecular graphics program for calculating and showing potential docking modes of a receptor and Schiff base ligand molecule. It required the input of the ligand and the receptor in PDB format. The water molecules, co-crystallized ligands, and other unsupported elements (such as Na, K, Hg, etc.) were eliminated while the amino acid chain was preserved. Gaussian03 software provides the Schiff base ligand structure in PDB file format. The Protein Data Bank (https://www.rcsb.org) provided download links for the crystal structures of many receptors.

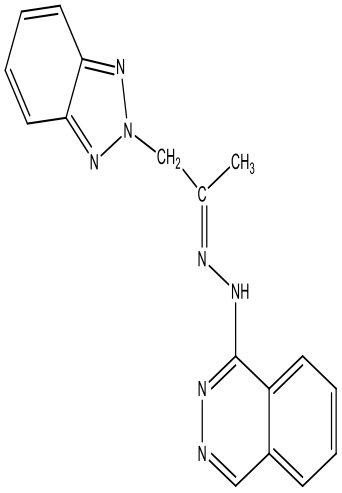

(*E*)-1-(2-(1-(2*H*-benzo[*d*][1,2,3]triazol-2-yl)propan-2-ylidene)hydrazinyl)phthalazine

Figure. 1: Structure of Schiff base ligand (L).

3.Results and Discussion

A freshly made L Schiff-base ligand, (E)-1-(2-(1-(2H-benzo[d][1,2,3]triazol-2-yl)propan-2-ylidene)hydrazinyl)phthalazine (Fig. 1), was submitted to elemental analysis, EI-mass, IR, UV-Vis, and ^{1}H NMR spectrum studies. The results of the elemental analyses (C, H, and N) are in good agreement with the suggested formulae in Table 1. The melting point of the Schiff base ligand (L) was extremely sharp, indicating high purity.

The mass spectra shown in Fig. 2 demonstrated a molecular ion peak at m/z 317, which is consistent with the molecular formula ($C_{17}H_{15}N_7$). The distinctive stretching vibration bands for NH, (C=N)azomethine, (C=N)phethalazine, Triazole ring stretching, and (N-N)triazol were visible in the IR data for the L ligand (Table 2) at 3259, 1629, 1584, 1573, and 1078 cm^{-1}, respectively [22, 33]. The absence of ketonic (CO) and amino (NH_2) bands along with the emergence of the azomethine (-C=N) stretching as a sharp band at 1629 cm^{-1} further supported the structure of the Schiff-base ligand.

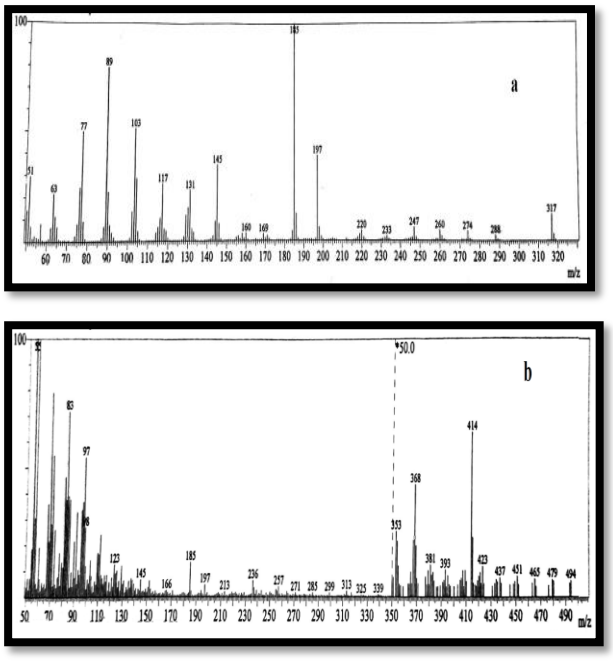

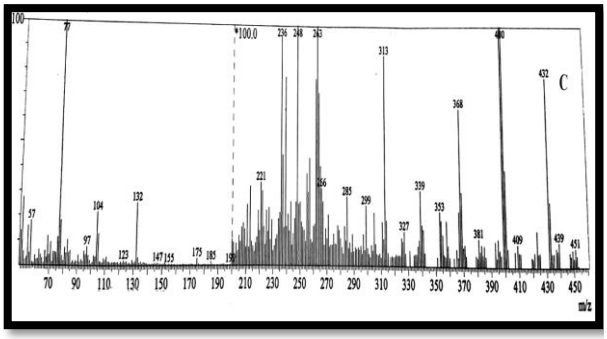

Figure. 2: Mass spectra of (a) Schiff base L, (b) [$CoLCl_2$], and (c) [$PdLCl_2$].

3.1.characterization of metal complexes

3.1.1.Elemental analyses and molar conductivity measurements

Complexes of Co(II) and Pd(II) are stable in the air. They are largely soluble in polar organic solvents including EtOH, MeOH, DMF, and DMSO. On the contrary, they cannot dissolve in water, though. Additionally, elemental analysis confirmed that the complexes have a metal/ligand ratio of 1:1. Besides, it was used to corroborate the stoichiometry and formulation of the Schiff base (L) ligand and its metal complexes. This was done by measuring the metal contents of the complexes as well as their carbon, hydrogen, nitrogen, and chlorine contents (Table 1). The ligand and their complexes' elemental studies show good agreement with the suggested structures. The complexes' molar conductivity values (Λm) in ethanol solvent (10^{-3}, M) at 25 ± 2 °C demonstrated that they were non-electrolytes. This demonstrated the chloride's attachment to the metal cations. The outcomes were compiled in Table 1.

Table 1: Physical and analytical data of Schiff base ligand (L) and its metal complexes

Compound (chemical formula)	Color Yield (%)	M.p. (°C)	Found (Calcd)				μ_{eff} (BM)	A_m (Ω^{-1} mol^{-1} cm^2)
			C (%)	H (%)	N (%)	M (%)		
L ($C_{17}H_{15}N_7$)	yellow (88)	180	64.25 (64.35)	4.56 (4.73)	30.59 (30.91)	–	–	–
[$CoLCl_2$]	Yellowish green (90)	160	45.31 (45.54)	3.04 (3.35)	21.58 (21.88)	12.97 (13.17)	3.28	15
[$PdLCl_2$]	Yellowish white (89)	225	41.02 (41.26)	2.89 (3.03)	19.68 (19.82)	21.11 (21.52)	Dia.	42

3.1.2.FT-IR spectroscopy

Table 2 displays the significant infrared absorption bands and spectra of L and its metal complexes. The characteristic vibrational frequencies, type, and intensity of the absorption bands are used to identify the functional groups that are present in the current Schiff bases. By contrasting the infrared spectra of the complexes with those of the corresponding free ligands, the sites of binding pertaining to the coordination of metal complexes and ligands have been examined (Tale 2). In the IR spectra of the ligand, the peaks corresponding to NH, (C=N)azomethine, (C=N)phethalazine, Triazol ring stretching, and (N-N)triazol were revealed at 3259, 1629, 1584, 1573, and 1078 cm^{-1}, respectively [22, 33–35]. The involvement of azomethine (C=N) was confirmed by the metal complex's IR spectra, where its band moved to 1642–1616 cm^{-1}. It was also decided to stretch (C=N) phethalazine at 1590 and 1576 cm^{-1}. The coordination of nitrogen from (azomethine and N-phethalazine) with the metal ions was demonstrated by the two complexes' appearance of new bands at 427 and 462 cm^{-1}. The triazole did not bind to the metal cations, as shown by the unchanged band of the ν(N-N) mode at 1088 cm^{-1} in the IR spectra of all the metal complexes [33–37]. According to our analysis of the IR spectra of the ligands and their metal complexes, the Schiff base L coordinates with the metal ions in a bidentate way, generating stable five-membered chelate rings around the metal ions through azomethine and phethalazine moiety nitrogen atoms.

Table 2: Prominent infrared frequencies (4000–400 cm^{-1}) of L and its metal complexes

Comound	*υ*(NH)	*υ*(C=N) *azomethine*	*υ*(C=N) *phethalazine*	*Triazol ring*	*υ* (N-N) *triazol*	*υ*(M–N)
L	3259sh	1629m	1584sh	1573s	1088sh	–
[CoLCl2]	3269sh	1616s	1576s	1539s	1089sh	462w
[PdLCl2]	3247sh	1642m	1590s	1536m	1088sh	427s

3.1.3.HNMR

The ligand (L) and its Pd(II) complex underwent ^{1}H-NMR spectroscopy measurements in the DMSO-*d6* solvent at room temperature (Table 3). The azomethine-NH proton was detected in the region of δ~ 5.92 ppm in the ^{1}H-NMR spectrum of L, while aromatic protons were detected in the range of δ~ 7.42 to 8.25 ppm [22]. At 8.98 ppm, a proton from the pyridazine ring emerged. The coordination of metal ions, which impact the signal positions, is confirmed by a minor shift in the NH proton signal and all aromatic proton signals when the chemical shift values of the ligand, L, and its Pd(II) complex are compared [38, 39].

3.1.4.Mass spectra

As seen in the spectra at m/z = 317 $[M]^+$ (L), 451 $[M+3]^+$ [$CoLCl_2$], and 494 $[M]^+$ [$PdLCl_2$], the present work used the ESI-MS technique to confirm the mass of the ligand, L, and its complexes [40, 41]. The molecular ions confirm a 1:1

stoichiometric ratio for metal to the ligand as properly determined by the ESI-MS data (Fig.2).

Table 3: ^{1}H NMR spectral data of the Schiff base ligand (L) and its Pd(II) complex

Compound	Chemical shift, (δ) ppm	Assignment
L	8.98	(s, H, CH *pyridazine*)
	7.42-8.25	(m, 8H, aromatic)
	5.92	(s, H, NH)
	5.62	(s, 2H, CH_2)
	1.93	(s, 3H, CH_3)
[$PdLCl_2$]	9.04	(s, H, CH *pyridazine*)
	7.39-8.22	(m, 8H, aromatic)
	6.01	(s, H, NH)
	5.59	(s, 2H, CH_2)
	1.91	(s, 3H, CH_3)

3.1.5.SEM

scanning electron microscopy (SEM) is a well-known and practical method for determining the surface morphology of produced substances. The physical appearances of the ligand and its metal complexes in SEM micrographs differ from one another [42, 43]. Fig. 3. displays the SEM images of L and its complexes. The Co(II) and Pd(II) complexes reveal an aggregate of non-uniform smaller globular-like structures of varying sizes, whilst the ligand L displays a small sponge-like structure with a rough surface. The ligand and its complexes range in size from 27 to 75 nm in nanometers.

3.1.6.Antimicrobial activity

For antibacterial and antifungal activity against certain Gram-positive (*Bacillus subtilis* and *Staphylococcus aureus*) and Gram-negative (*E. Coli* and *Neisseria gonorrhoeae*) bacterial strains as well as *Candida alibicans* fungal species, the synthesized ligand and its metal(II) complexes were tested. Table 4 lists the antibacterial and antifungal activity observations. The observed outcomes demonstrate that both Gram-positive and Gram-negative bacterial strains are susceptible to the complexes of the current investigation (Fig.4). The Co(II) complex showed excellent activity against all bacterial strains, particularly *Staphylococcus aureus*, although it did not affect the fungus *Candida alibicans*. Based on the chelation theory, the stronger antibacterial activity of the produced metal(II) complexes than the Schiff base reported here can be well explained [44–48].

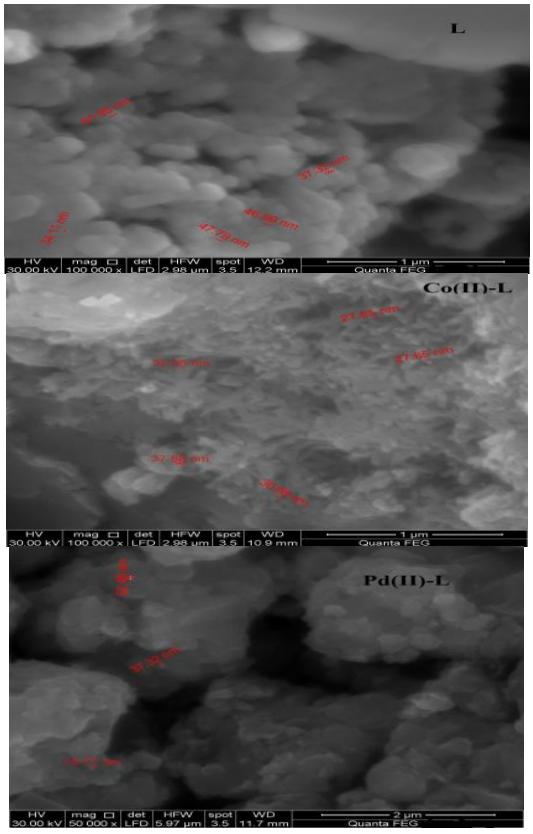

Figure. 3: Scanning electron microscope images of Schiff base ligand (L) and its metal complexes.

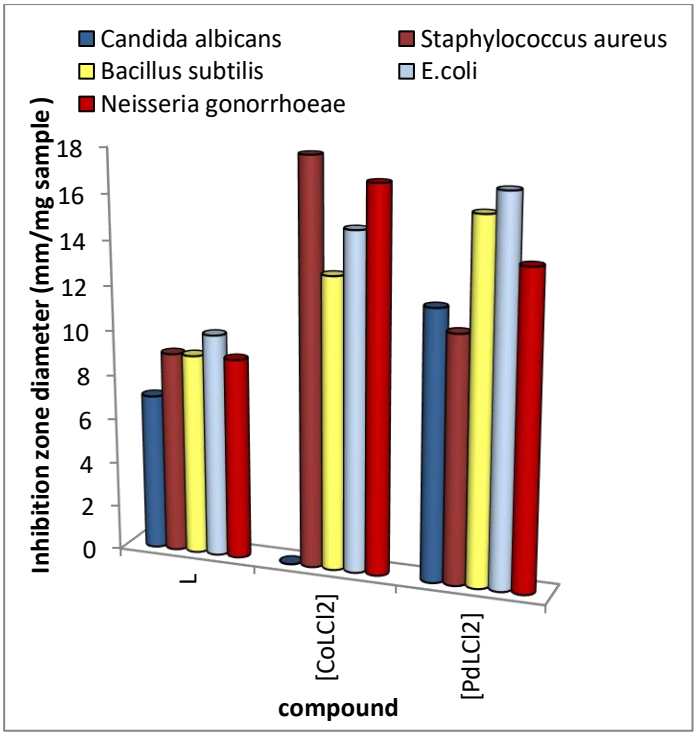

Figure. 4: Biological activity of Schiff base ligand and its metal complexes against different bacterial and fungal species.

Table 4: Biological activity of L ligand and its metal complexes

Sample	Inhibition zone diameter (mm / mg sample)				
	Gram positive bacterial species		Gram negative bacterial species		Fungi
	Bacillus subtilis	*Staphylococcus aureus*	*E.coli*	*Neisseria gonorrhoeae*	*Candida alibicans*
L	**9**	**9**	**10**	**9**	**7**
[$CoLCl_2$]	**13**	**18**	**15**	**17**	**NA**
[$PdLCl_2$]	**16**	**11**	**17**	**14**	**12**
Ampi-cillin	**26**	**21**	**25**	**28**	-----
Ampho-tericin B	-----	-----	-----	-----	**21**

NA: no activity
Ampicillin: Standard antibacterial agent; Amphotericin B: Standard antifungal agent.

3.1.7.In vitro antitumor activities

The tested compounds' in-vitro cytotoxic effects on the MCF-7 and HepG2 tumour cell lines were assessed over concentration. The tested substances varied in their ability to kill human tumour cells. Palladium complex was shown to have the greatest toxicity against the cell lines MCF-7 and HepG2, with IC_{50} values of 20.23 and 48.54, respectively, (Fig.5). Notably, the complexation of the ligand to the metal ions increased the anticancer action [49–52]. It was discovered that the Ligand had the lowest cytotoxicity against the MCF-7 and HepG2 cell lines (Table 5).

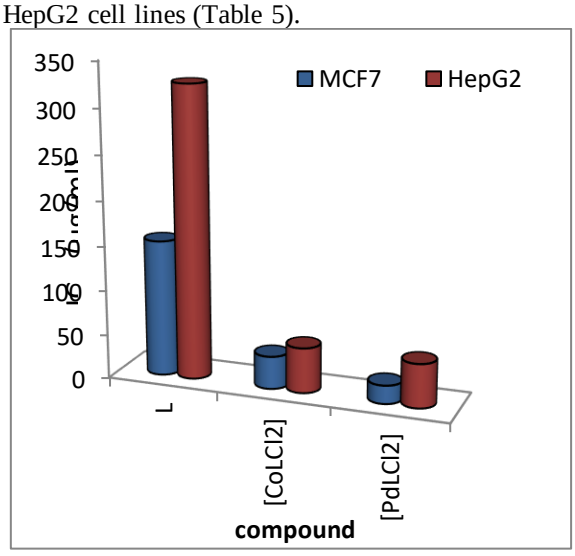

Figure. 5: IC_{50} of Schiff base (L) with breast (MCF7) and liver (HepG2) cancer cell lines

Table 5: Anti-breast cancer activity of L ligand and its metal complexes against breast cancer cell line (MCF7) and liver cancer cell line (HepG2)

Compound	IC_{50} (µg/ml)	
	MCF7	**HepG2**
L	152	326
[$CoLCl_2$]	36.18	50.01
[$PdLCl_2$]	20.23	48.54

3.1.8.Molecular docking studies

Antibacterial and antifungal activities

The crystal structure of *Staphylococcus aureus* (3Q8U), the crystal structure of *E. coli* (3t88), and the fungus *Candida albicans* (5JPE) were docked with the Schiff base (L), which show how well these receptors bind to their respective ligand molecules (Table 6). Protein receptors that are attracted to L mostly form H-bonding or π-bonding interactions at their active regions [51–53]. According to the results of the molecular docking, the L molecule had stronger binding energies with the *Candida albicans* fungus's 5jpe receptor, reaching -4.2 kcal/mol. The L compound's 2D and 3D molecular interactions are depicted in Fig. 6.

Receptor	2D	3D
3HB5	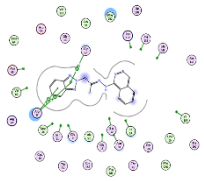	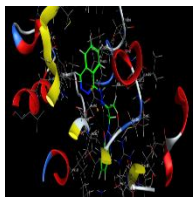
3Q8U	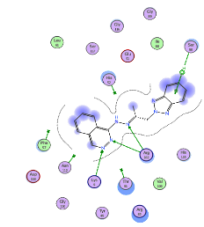	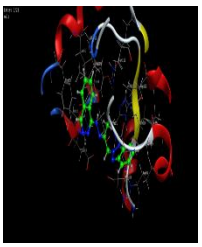
3T88	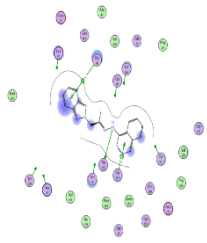	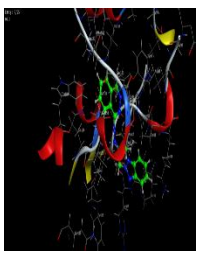

5jpe	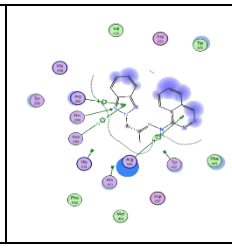	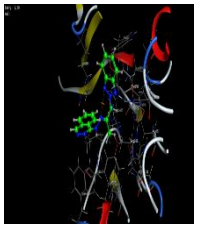

Figure. 6: The interaction between Schiff base ligand (L) and different receptors in 2D and 3D images.

Table 6: Interaction energy values obtained from docking calculations of L ligand with receptors of crystal structure of nucleoside diphosphate kinase of *Staphylococcus aureus* (3Q8U), crystal structure of *E.coli* (3t88), protein phosphatase of fungus *Candida albicans* (5JPE) and with crystal structure of breast cancer receptor (3HB5)

Receptor	Ligand moiety	Receptor site	Interaction	Distance (A°)	E (kcal/mol)
3HB5	6-ring	NE ARG 37	pi-cation	4.03	-0.8
	5-ring	NH2 ARG 37	pi-cation	3.69	-3.3
	5-ring	N GLY 92	pi-H	4.03	-3.2
3Q8U	N 25	NH2 ARG 102 (A)	H-acceptor	3.28	-1.0
	N 26	NZ LYS 9 (A)	H-acceptor	2.81	-0.8
	N 37	NH1 ARG 102 (A)	H-acceptor	3.22	-1.0
	N 37	NH2 ARG 102 (A)	H-acceptor	3.35	-2.6
	6-ring	CA SER 90 (A)	pi-H	4.03	-1.2
3T88	N 38	OG1 THR 155 (A)	H-donor	2.87	0.3
	6-ring	N GLN 88 (A)	pi-H	4.50	-0.6
	6-ring	N GLY 133 (A)	pi-H	3.65	-0.7
5Jpe	N 11	NE2 HIS 290 (A)	H-acceptor	3.10	-4.2
	5-ring	NH2 ARG 261 (A)	pi-cation	4.35	-0.9
	5-ring	ND2 ASN 289 (A)	pi-H	4.37	-1.2
	6-ring	NH1 ARG 386 (A)	pi-cation	3.89	-2.7

3.1.9.Anticancer activity

The crystal structure of the breast cancer receptor was docked with the Schiff base ligand (L) (3HB5). Fig.6. displays the 2D and 3D interactions. The major mode of engagement is through π-bonding. With the help of the data in Table 6, we were able to determine that the L molecule had a promising binding affinity of -3.3 kcal/mol.

Conclusion

The Schiff base (E)-1-(2-(1-(2H-benzo[d][1,2,3]triazol-2-yl)propan-2-ylidene)hydrazinyl)phthalazine has been used as a starting point for the synthesis of cobalt and palladium chelates. In chelates of Co(II) and Pd(II), the ligand L functions as a neutral bidentate. It was clear from the antibacterial activity of all chelates that the complexes were more effective than the parent ligand. The antibacterial behavior is thus significantly impacted by metal chelation. Following the chelation principle, the antibacterial activity has become clear. The Pd(II) complex is one of the produced chemicals that has the most potential as a powerful antifungal agent. In comparison to all tested cancer cell lines, the Pd(II) chelate also shows stronger anticancer activity. The biological activities of the synthesized compounds against organisms have shown promise trend, but more extensive research on both humans and animals is required. The 5jpe receptor of the fungus *Candida albicans* has the highest binding affinity for L, with a binding energy of -4.2 kcal/mol, as demonstrated by the molecular docking analysis with other receptors.

Conflict of interest

There are no conflicts to declare.

Funding source

No funding source is present

3. References

1. N. Raman, A. Selvan, S. Sudharsan, Spectrochim Acta A 79 (2011) 873–883.
2. K.E. Erkkila, D.T. Odom, J.K. Barton, Chem. Rev 99 (1999) 2777–2796.
3. B.L Fei, W.S. Xu, H.W Tao, W. Li, Y. Zhang, J.Y. Long, Q.B. Liu, B. Xia, W.Y., J. Photochem. Photobiol. B: Biology 132 (2014) 36–44.
4. P.K. Sasmal, A.K. Patra, A.R. Chakravarty, J. Inorg. Biochem. 102 (2008) 1463–1472.
5. Y. Gou, J. Li, B. Fan, B. Xu, M. Zhou, F. Yang, Eur. J. Med. Chem 134 (2017) 207–217.
6. A.M. Pyle, T. Morii, J.K. Barton, J. Am. Chem. Soc. 112 (1990) 9432–9434.
7. M. Howe-Grant, S.J. Lippard, Biochemistry 18 (1979) 5762–5769.

8. S. Layeka, R. Gangulyb, D.D. Pathaka, J. Organometal. Chem. 870 (2018) 16–22.
9. H.P. Ebrahimi, J.S. Hadi, Z.A. Abdulnabi, Z. Bolandnazar, Spectrochimica Acta Part A, Mol. and Biomol. Spectr 117 (2014) 485–492.
10. D.S. Shankar, A. Rambabu, N. Vamsikrishna, N. Ganji, S. Daravath, Shivaraj, Inorg. Chemi. Commu 98 (2018) 48–57.
11. V.K. Gupta, A.K. Singh, S. Mehtab, B. Gupta, Anal. Chimica Acta 566 (2006) 5–10.
12. S.M. Pradeepa, H.S. Bhojya Naik, B. Vinay Kumar, K. Indira Priyadarsini, Atanu Barik, T.R. Ravikumar Naik, Spectrochimica Acta Part A: Mol. and Biomol, Spectr 101 (2013) 132–139.
13. Alhadhrami, A., et al. Materials, 2022. 15(22): p. 8211.
14. B.S. Garg, Deo Nandan Kumar, Spectrochimica Acta Part A 59 (2003) 229–234.
15. R.N. Patel, S.P. Rawat, M. Choudhary, V.P. Sondhiya, D.K. Patel, K.K. Shukla, D.K. Patel, Y. Singh, R. Pandey, Inorg. Chimica Acta 392 (2012) 283–291.
16. A.A. El-Sherif, A. Fetoh , Yasir Kh. Abdulhamed , G. M. Abu El-Reash, Inorg Chim. Acta 480 (2018) 1–15.
17. G.A.M Elhagali, G.A Elsayed, R.A. Eliswey, A.A. El-Sherif, J of the Iranian Chemical Society,15(6) (2018) 1243-1254.
18. A. I. Vogel, Quantitative Inorganic Analysis Including Elemental Instrumental Analysis, 2nd ed., Longmans, London, 1962.
19. A.T. Abdelkarim, W.H. Mahmoud, A.A. El-Sherif, Journal of Molecular Liquids, 328 (2021) , 115334.
20. Albert, A., Selective Toxicity, New York: Wiley, 1979.
21. J. Zhang, L. Xu, W. Wong, Coord. Chem. Rev. 335 (2018) 180-198.
22. A. Rambabu, N. Ganji, S. Daravath, K. Venkateswarlu, K. Rangan, Shivaraj, J Mol. Str.1199 (2020) 127006.
23. M. Hong, G. Chang, R. Li, M. Niu, New J. Chem. 40 (2016) 7889-7900.
24. A. Rambabu, M.P. Kumar, S. Tejaswi, N. Vamsikrishna, Shivaraj, J. Photochem. Photobiol. B Biol. 165 (2016) 147-156.
25. S. Chandra, D. Jain, A. K. Sharma, P. Sharma, Molecules 14 (2009) 174.
26. K.A. Asla, A.T. Abdelkarimm, G.M.A El-Reash, A.A. El-Sherif, International Journal of Electrochemical Science, 15 (2020) 3891-3913.
27. P. Skehan, R. Storeng, D, Scudiero, A. Monks, J. McMahon, D. Vistica, J. T. Warren, H. Bokesch, S. Kenney, M. R. Boyd, J. Nati. Cancer Inst. 82 (1990) 1107.
28. A.A. El-Sherif, M.M. Shoukry, A.T. Abd Elkarim, M.H. Barakat, Bioinorganic Chemistry and Applications, 2014 (2014) 626719.
29. M. M Abd-Elzaher, A. A. Labib, H. A. Mousa, S. A. Moustafa, M. M. Ali, A. A El-Rashedy, J. Bas. App. Sci. 5 (2016) 85.
30. A.A. El-Sherif, M.R. Shehata, M.M. Shoukry, N.M. Mahmoud, Journal of Molecular Liquids, 262(2018) 422-434
31. D. D. Patel and K. R. Patel, Materials Today: Proceedings (2021) article in press.
32. A.M. Hassan, B. H. Heakal, A. Younis, M. A. Bedair, Z. I. Elbialy and M. M. Abdelsalam, Egypt.J.Chem. 62, 9 (2019) 1603 – 1624.
33. C. Richardson and P.J. Steel, D a l t o n T r a n s ., (2 0 0 3) 9 9 2 – 1 0 0 0.
34. S. Roggan, C. Limberg, C. Knispel and T. Don Tilley, Dalton Trans.,40 (2011) 4315
35. Emad S. Mousa, Walaa H. Mahmoud, Appl Organometal Chem. 33:e4844 (2019) 1-18.
36. H. Kargar, V. Torabi, A. Akbari, R. Behjatmanesh-Ardakani, A. Sahraei, M. N. Tahir, J Molr Str, 1205 (2020) 127642.
37. G. Ramesh, S. Daravath and M. Swathi V. Sumalatha, D. S. Shankar, Chem. Data Collections 28 (2020) 100434.
38. El-Karim, A.T.A. El-Sherif, A.A. Journal of Molecular Liquids219(2016)914-922
39. I. Belkhettab, S. Boutamine, H. Slaouti, M. F. Zid, H. Boughzala , Z. Hank al, J Mol Str 1206 (2020) 127597.
40. Ahmed A. Soliman, Mina A. Amin, Ahmed A. El-Sherif, Cigdem Sahin, Canan Varlikli**,** Arabian Journal of Chemistry**,**Volume 10, Issue 3**,** (2017)Pages 389-397.
41. G.A.M Elhagali, G.A Elsayed, R.A. Eliswey, A.A. El-Sherif, J Iran Chem Soc15 (2018) 1243-1254.
42. W. H. Mahmoud, R. G. Deghadi, G. G. Mohamed, India. J. Chem.58 (2019) 1319.
43. A. M. A. Alaghaz, M. E. Zayed, S. A. Alharbi, J. Mol. Str. 1048 (2015) 36.
44. C. Justin Dhanaraj, M. Jebapriya, C.J. Dhanaraj, M. Jebapriya, J Mol Str, 1220 (2020) 128596.
45. A. Chaudhary, R.V. Singh, Phosphorus, Sulfur, Silicon Relat. Elem. 178 (2013) 603-613.
46. B.G. Tweedy, Phytopathology 55 (1964) 910.
47. M.S. Aljahdali, A.A El-Sherif, Bioinorganic Chemistry and Applications, 2020,2020, 8866382.
48. A.A. El-Sherif, A.A El-Sisi, M. Ali, O. AlTaweel, A.T AbdEl-Karim, International Journal of Electrochemical Science, 15(11)(2020) 10885-10907.
49. S.E. Abd El-Razek, S. M. El-Gamasy, M. Hassan, M.S. Abdel-Aziz, S.M. Nasr, J Mol. Str. 1203 (2020) 127381.
50. A.N. Al-Hakimi, F. Alminderej, L. Aroua, S. K. Alhag M.Y. Alfaifi, O.M. Samir, J.A.

Mahyoub,S. I. Elbehairi , A.S. Alnafisah, Arab. J. Chemistry (2020), https://doi.org/10.1016/j.arabjc.2020.08.014
51. A.A. El-Sherif, M.M. Shoukry, L.O Abobakr, Spectrochimica Acta - Part A: Molecular and Biomolecular Spectroscopy, 112(2013) 290-300.
52. M. M Abd-Elzaher, A. A. Labib, H. A. Mousa, S. A. Moustafa, M. M. Ali, A. A El-Rashedy, J. Bas. App. Sci. 5 (2016) 85.
53. L. A. Anthony , D. Rajaraman , M. Shanmugam, K. Krishnasamy, Chem. Data Collections 28 (2020) 100421.